NEW APPROACHING IN NEUTRON ABSORPTION ON $TH_XSR_2O_{1.8}$ NANO MATERIAL STRUCTURE WITH QUANTUM DOT AT MAGNETIC QUADRUPOLE ENHANCEMENT

Moh. Hardiyanto
Betha Group Large Hadron Collider Laboratory, CERN – Lyon, France
Alpha Section Muon Accelerator Max Planck Institute – Damstadt, Germany
Industrial Engineering Department – ITI Serpong, Indonesia
E-mail : moh_hardiyanto_iti@yahoo.com

ABSTRACT

We present a theoretical investigation of $Th_xSr_2O_{1.8}$ nano material structure with quantum dot interacting with a strongly localized optical field as encountered in high-resolution near-field optical microscopy. The strong gradients of these localized fields suggest that higher-order multipolar interactions will affect the standard magnetic dipole transition rates and selection rules. For neutron tunneling quantum dot in the strong confinement limit we calculated the interband magnetic quadrupole absorption rate and the associated selection rules. Founded that the magnetic quadrupole absorption rate is comparable with the absorption rate calculated in the magnetic dipole approximation. This implies that near-field optical techniques can extend the range of spectroscopic measurements for 412 MHz at quantum magnetic field until 515 MHz deployment quantum field at $\vec{B}$ around 375-450 tesla beyond the standard dipole approximation. However, we also show that spatial resolution cannot be improved by the selective excitation of electric quadrupole transitions.

Keywords: *neutron interband, $Th_xSr_2O_{1.8}$ nano material structure, quantum dot, magnetic quadrupole*

INTISARI

Kami mempresentasikan suatu penyelidikan teoritik dari struktur nano material *Th_xSr_2O* dengan adanya interaksi *quantum-dot* melalui suatu medan optik yang dilokasikan secara amat kuat sebagai pengukuran pada medan terdekat dalam mikroskopi optikal. Beberapa *gradien* kuat pada medan-medan yang dilokasikan tersebut memperlihatkan ragam interaksi *multipolar* berorde amat tinggi sehingga akan menimbulkan efek rata-rata transisi pada dipol magnet standar dan aturan seleksi magnetik yang ada. Untuk penerobosan *quantum-dot* netron dalam batasan terukur yang kuat kami mengkalkulasikan adanya *interband* nilai rata-rata absorpsi *magnetic-quadrupole* dan hal lainnya pada aturan-aturan seleksi. Ditemukan bahwa nilai rata-rata absorpsi *magnetic-quadrupole* dapat diperbandingkan dengan hasil nilai rata-rata kalkulasi pada pendekatan dalam absorpsi *magnetic-dipole* yang diteliti. Melalui aplikasi optikal pada medan yang ada yaitu *magnetic-dipole* dengan memperluas pengukuran-pengukuran spektroskopi pada medan *quantum-magnetic* sebesar 412 MHz sampai 515 MHz dengan menguraikan medan kuantum di $\vec{B}$ sekitar 375-450 tesla berlandaskan pada pendekatan dipol standar. Hal lainnya, kami juga memperlihatkan adanya resolusi terpisah yang tidak dapat ditingkatkan melalui eksitasi selektif dari adanya transisi listrik pada *quadrupole* yang ada.

Kata kunci : *interband* netron, struktur nano material *$Th_xSr_2O_{1.8}$* , *quantum-dot* , *magnetic-quadrupole*

INTRODUCTION

Near-field optical techniques based on quantum approximation have extended the range of optical measurements beyond the diffraction limit and stimulated interest in many disciplines, especially in material sciences. The increase of spatial resolution is achieved by access to evanescent modes in the electromagnetic field. These modes are characterized by high spatial frequencies and therefore permit the probing of sub wavelength structures. Near-field optical techniques have also been employed for the study of optical properties and dynamics of charge carriers in artificial nano structures such as quantum wells, quantum wires, and quantum dots (A. Knorr, et all, 2013).

In this paper we focus on the interaction of a spherical of $Th_xSr_2O_{1.8}$ nano material structure with quantum dot a highly confined optical near field. It has been shown that such fields can be generated near laser-illuminated sharply pointed tips. Adopt this geometry and approximate the fields near the

tip by an oscillating magnetic dipole oriented along the tip axis. In the research reported it was demonstrated that this is a reasonable approximation and that the dipole moment can be related to the computationally determined field enhancement factor using by Volkov's detector and Multi Channel Spectroscopy Nuclear Beam at Betha Goup CERN nuclear reactor.

Figure 1. Volkov's detector
(Courtesy of Betha Group LHC CERN, Lyon, France, 2014)

The interaction between a quantum dot and the optical near field is described semi classically by use of the multipolar expansion. Our study for the answers to two basic questions: (1) to what extent are standard selection rules modified by higher-order multipolar neutron transitions in confined optical fields and (2) can optical resolution be improved by selective excitation of higher-order multipolar neutron transitions.

Literature Review

A. Multipolar Hamiltonian

A semi classical approach to describe the interaction of a quantum dot with the electromagnetic field. In this approach the electromagnetic field obeys Maxwell's equations, and the Hamiltonian of the system ($\hat{H}$) can be separated into two contributions as (E.J. Sanchez, et. all., 2013)

$$\hat{H} = \hat{H}_0 + \hat{H}_I \quad (1)$$

where $\hat{H}_0$ and $\hat{H}_I$ are the unperturbed Hamiltonian (absence of fields) and the interaction Hamiltonian, respectively. In the Coulomb gauge they are defined as

$$\hat{H}_0 = \frac{1}{2m}\hat{p}^2 + V(r) \quad (2)$$

$$\hat{H}_I = -\frac{e}{m}\hat{p}.A(r,t) + \frac{e^2}{2m}A^2(r,t) + e\phi(r,t) \quad (3)$$

where *V(r)* is the potential energy, $\hat{p}$ is the canonical momentum, A(r, t) is the vector potential, and ϕ(r, t) is the scalar potential. The multipolar Hamiltonian is obtained by use of canonical-transformation $\hat{U} = \exp(i\,z/\hbar)$, in which *z* is given by

$$z = \int \tilde{P}(r).A(r,t)d^3r \equiv 0 \quad (4)$$

where $\tilde{P}(r)$ is the polarization. If vector potential A(r, t) and scalar potential ϕ(r, t) are expanded in a Taylor series with respect to a reference charge distribution at R, as follows:

$$A(r,t) = \sum_{n=0}^{\infty} \frac{1}{(n+2)n!}[(r-R).\nabla]^n B(R,t) \times (r-R) \quad (5)$$

d, m, and $\overleftrightarrow{Q}$ are the electric dipole moment, the magnetic dipole moment, and the magnetic quadrupole moment, respectively, with respect to a reference charge distribution at R. Nabla operator ∇_1 acts only on the spatial coordinates r_1 of the magnetic field. It is important to mention that *m* depends on the canonical momentum. However, for weak fields the canonical momentum can be approximated as the mechanical momentum.

B. Quantum Dot Wave Functions (Strong Confinement)

We assume that a spherical quantum dot is made from a direct band gap conductor for which the bulk magnetic dipole transitions are allowed between the valence band and the conduction band. In a generic manner we assume that the valence band has a *p*-like character and that the conduction band has an *s*-like character. The latter assumption is commonly encountered for several conductors such as $Th_xO_{1.7}$. We also assume that an electron and a hole are completely confined in a sphere with radius *a* by the potential energy

$$V(r) = \begin{cases} 0 & r \le a \\ \infty & r > a \end{cases} \quad (6)$$

where *r* is the radial coordinate. Also, that the electron (hole) has the same effective mass $m_e(m_h)$ as in the bulk material. This assumption is valid if the volume of the sphere is much larger than the volume of a primitive cell in the crystal. Strong confinement is achieved if the Bohr radii of electron b_e and b_h hole are much larger than the radius of the quantum dot. By assuming the mentioned conditions can express the wave function of the electron in the conduction band as

$$\Psi^E(r) = \frac{1}{\sqrt{V_0}} u_{c,0}(r)\xi^e(r) \quad (7)$$

Here $u_{c,0}(r)$ is the conduction band Bloch function (with lattice periodicity) that has the corresponding eigenvalue *k* = 0, and V_o is the volume of the unit cell. If this energy difference is much larger than Coulomb interaction $e^2/(4\pi\varepsilon_o \in a^2)$, the electron hole interaction can be neglected. Under this assumption, envelope function $\zeta^{e(h)}(r)$ for the electron (hole) satisfies the time-independent Schrödinger equation in which the potential energy is given by Eq. (5). The solution in spherical coordinates (r,θ,ϕ) is given by

$$\xi^{e(h)}_{n,l,m}(r,\theta,\phi) = \Lambda_{nl}(r)Y_{l,m}(\theta,\phi) \quad (8)$$

Here $Y_{l,m}(\theta,\phi)$ are the spherical harmonics, and the radial function $\Lambda_{nl}(r)$ is

$$\Lambda_{nl}(r) = \sqrt{\frac{2}{a^3}} \frac{1}{j_{l+1}(\beta_{nl})} jl\left(\beta_{nl}\frac{r}{a}\right) \quad (9)$$

j_l is the *l* th-order spherical Bessel function and β_{nl} is the *n* th root of j_l , that is, $j_l(\beta_{nl})$ =0 .

C. Field Operator Representation

The annihilation carrier field operator $\{\hat{\Psi}\}$ can be expressed as a linear combination of hole creation operators in the valence band and electron annihilation operators in the conduction band.

$$\hat{\Psi}(r) = \sum_{n,l,m}\left[\frac{1}{\sqrt{V_0}} u_{v,o}(r)\xi^h_{nlm}(r)\hat{g}^+_{nlm}\right] \quad (10)$$

$\hat{f}_{nlm}$ is the annihilation operator for an electron in the conduction band with envelope function $\zeta^e_{nlm}(r)$; $\hat{g}^+_{nlm}$ is the creation operator for a hole in the valence band with envelope function $\zeta^h_{nlm}(r)$. Creation carrier field operator $\hat{\Psi}^+$ is the adjoint of Eq. (8).

METHODOLOGY

A. Electric Quadrupole Hamiltonian

The magnetic quadrupole interaction Hamiltonian $\hat{H}^Q$ can be represented as

$$\hat{H}^Q = \hat{\Psi}^+(r)H^Q(r)\hat{\Psi}(r)d^3r \quad (11)$$

$$\hat{H}^Q(r) = -\nabla_1 \cdot \vec{\vec{Q}}(r)B(r_1,t)\big|_{r1=0} \quad (12)$$

Here and in what follows, the subsequent listing of two vectors [as in Eq. (9)] denotes the outer product (dyadic product). The interband terms are found by substitution of Eq. (10) and its adjoint into Eq. (11), thus (Levy, V., et. all, 2013):

$$\hat{H}^Q = -\nabla_1\left[\sum_{nlm}\sum_{rst}\hat{f}^+_{nlm}\hat{g}^+_{rst}\int u^*_{c,0}(r)\zeta^*_{nlm}(r) \times \vec{\vec{Q}}(r)u_{v,0}(r)\zeta^h_{rst}(r)d^3r - \right]B(r_1,t)\big|_{r_1=0} + h.c., \quad (13)$$

where (*h.c.*) denotes the Hermitian conjugate. We calculate the integral on the right-hand side of Eq. (12) by decomposing it into a sum of integrals over the volume occupied by each of the unit cells. Applying the coordinate transformation $r' = r - R_q$, where R_q is a translational lattice vector (the lattice remains unchanged when it is translated by R_q), yields.

The term containing R_qR_q has vanished because of the orthogonality of the Bloch functions, i.e.,

$< u_{i,0} \left| u_{j,0} >= \tilde{\delta}_{ij}; i, j = c, v. \overleftrightarrow{Q}_{cv}$ vanish because we are assuming that the valence band is *p* like and the $\overleftrightarrow{Q}_{cv} = 0$ conduction band is *s* like.

B. Magnetic Quadrupole Selection Rules and Absorption Rate

Using the Fermi Golden Rule yields the magnetic quadrupole transition rate $\left(\alpha^{Q}\right)$ for photon absorption:

$$\alpha^{Q} = \frac{2\pi}{\hbar} \sum_{nlm} \sum_{rst} \left| \left\langle nml; rst \left| \hat{H}_{\text{int}}^{Q} \right| 0 \right\rangle \right|^2 \delta \left[\hbar\omega - (\varepsilon_{nl}^{e} + \varepsilon_{rs}^{h})\right] \quad (14)$$

Here $\left|0\right\rangle$ is the ground state of the quantum dot. By substituting Eq. (12) into Eq. (13) we obtain the electric quadrupole transition rate.

$$\alpha^{Q} = \frac{2\pi}{\hbar} e^2 \sum_{nlm} \sum_{rst} \left| \nabla_1 \cdot (\tfrac{1}{2} P_{cv} D_{nmlrst} + \tfrac{1}{2} D_{nmlrst} P_{cv}) \tilde{B}(r_1) \right|_{r1=0}^{2} \delta[\hbar\omega - (\varepsilon_{nl}^{e} + \varepsilon_{rs}^{h})] \quad (15)$$

We find that the magnetic quadrupole absorption rate contains the dyadic product of P_{cv} and D_{nmlrst}. Whereas P_{cv} depends on the bulk material properties, D_{nmlrst} depends on the quantum dot properties.

C. Absorption Rates in $Th_xSr_2O_{1.8}$ Micro Structure

To compare the magnetic dipole and the magnetic quadrupole absorption rates in strongly confined optical fields consider a quantum dot in the vicinity of a laser-illuminated metal tip. The strongest light confinement is achieved when the metal tip is irradiated with light polarized along the tip's axis. For this situation

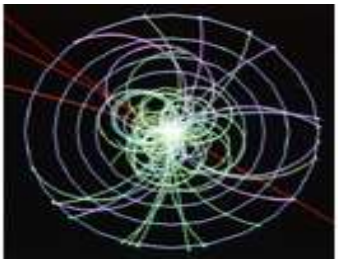

Figure 2 illustrates the comparison of $Th_xSr_2O_{1.8}$ nano material structure in magnetic dipole and magnetic quadrupole (Courtesy of Betha Group LHC CERN, Lyon, France, 2014)

Figure 2 shows field distribution $\left(\left|B\right|^2\right)$ rigorously calculated by the multiple multipolar method 20 near a gold tip with a 10 nm end diameter and irradiated with 700 nm light. In the multiple multipolar neutron method, electromagnetic fields are represented by a series expansion of known analytical solutions of Maxwell's equations. The calculated field distribution for our particular geometry can be well approximated by the field generated by magnetic dipole aligned along tip axis *z* and located at the origin of tip curvature. The only adjustable parameter is dipole moment P_o, which can be related to the computationally determined field enhancement factor in $Th_xSr_2O_{1.8}$ nano material structure.

To calculate magnetic quadrupole absorption rate $\left(\alpha^{Q}\right)$ and magnetic dipole absorption rate $\left(\alpha^{B}\right)$ we consider Bloch functions for the valence band and the conduction band that are similar to those of $Th_xO_{1.7}$. If we ignore spin–orbit coupling and spin degeneracy, the *p*-like valence band is threefold degenerate. $Th_xSr_2O_{1.8}$ nano material structure has a lattice constant of *d* = 0.565 nm, and the effective masses of electron and hole are m_e= 50.067m_o and m_h = 50.080m_o (light hole), respectively. Inclusion of the heavy hole will shift the hole energy levels only as long as the heavy-hole Bohr radius is larger than the quantum dot radius.

The lowest allowed magnetic dipole transition, the transition with the lowest allowed energy difference between initial and final states at 375 - 410 tesla magnetic field.

Analysis and Discussion of the $Th_xSr_2O_{1.8}$ Nano Material Structure with Quantum Dot

We analyze absorption rates for quantum dots with the two different radii, *a* = 5 nm and *a* = 10 nm. For *a* = 5 nm the magnetic quadrupole transition is excited at a wavelength of $\lambda \approx 500$ nm; the magnetic dipole transition, at $\lambda \approx 550$nm. The quadrupole transition for a quantum dot of radius *a* = 10 nm occurs at $\lambda \approx 615$ nm, and the magnetic dipole transition at $\lambda \approx 630$ nm.

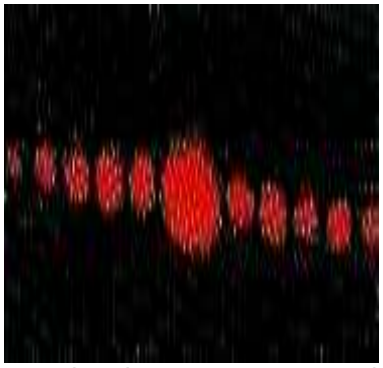

Figure 3 The $Th_xSr_2O_{1.8}$ nano material structure
at 395 - 405 tesla magnetic field after blasting by neutron absorption in 1.9 x 10^5 currie/mm
(Courtesy of Betha Group LHC CERN, Lyon, France, 2014)

For a quantum dot that is just beneath the exciting dipole **(r** = 0), the vertical dashed lines indicate the minimum physical distance between the quantum dot and the dipole, i.e., the limit at which the tip and the quantum dot would touch (we assume a tip radius of 5 nm).

For the quantum dot with radius *a* = 5 nm and an excitation wavelength of $\lambda \approx$ 550 nm the normalized minimum distance is $z_o^{min} / \lambda \approx 0.018$. Similarly, for the quantum dot with radius *a* = 10 nm and a wavelength of $\lambda \approx 630$ nm the minimum distance is 15 nm, which corresponds to a normalized distance of $z_o^{min} / \lambda \approx 0.024$. The important finding is that the ratio $\langle \alpha^Q \rangle / \langle \alpha^B \rangle$ can be as high as 0.3 for a 5-nm quantum dot and even 0.6 for a 10-nm quantum dot. These values are roughly 3 orders of magnitude larger than those obtained by use of far-field excitation [for plane-wave excitation the ratio is of the order of $(a/\lambda)^2$]. Thus we find that, in the extreme near field $(z_o < \lambda/10$, quadrupole transitions become important and the magnetic dipole approximation is not sufficiently accurate.

We generated the plots in Figs. 4 by scanning the quantum dot in the *xy* plane while keeping the exciting dipole at constant height z_o .

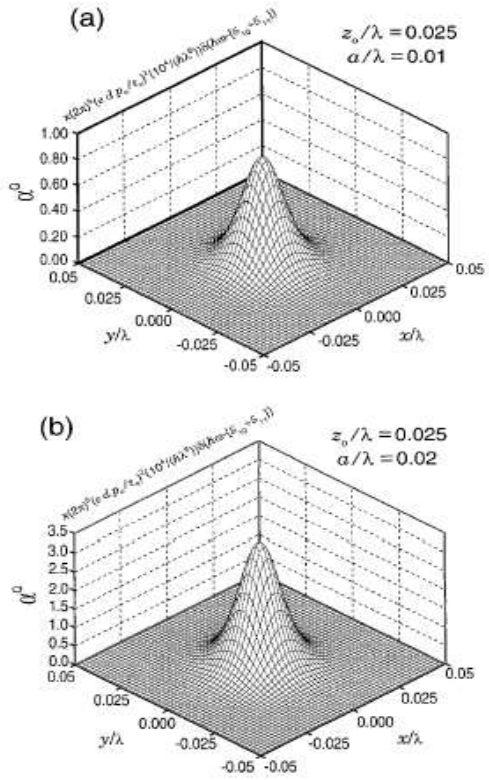

Fig. 4 shows the magnetic quadrupole absorption rate $\langle \alpha^Q \rangle$ from $Th_xSr_2O_{1.8}$ nano material structure at 405 tesla magnetic field
after blasting by neutron absorption in 1.9 x 10^5 currie/mm
(Courtesy of Betha Group LHC CERN, Lyon, France, 2014)

Both plots are symmetrical with respect to the *z* axis. For $\langle \alpha^B \rangle$ this symmetry is generated by the dominant field component $\tilde{B}_z$, whereas for $\langle \alpha^Q \rangle$ the symmetry is due to the strong field gradient $\partial \tilde{B}_z / \partial z$. The magnetic dipole absorption rate is proportional to the square of the particle dipole moment p_o and to the square of the lattice constant of the crystal *d* in $Th_xSr_2O_{1.8}$ nano material structure. The quadrupole absorption rate is also proportional to the square of (a/λ), as is evident, where the ratio a/λ is twice the ratio a/λ .

CONCLUSIONS

We have analyzed higher-order multipolar neutron absorption interactions between $Th_xSr_2O_{1.8}$ nano material structure with quantum dot and a strongly confined optical field. Expressions have been derived for the electric quadrupole interaction Hamiltonian, the associated absorption rate, and selection rules. It has been assumed that the quantum dot has a *p*-like valence band and an *s*-like conduction band. The magnetic quadrupole absorption strength depends on the bulk properties of the material (Bloch functions) as well as on the envelope functions (confinement functions).

When the quantum dot with radius *a* interacts with the confined optical field produced by a sharply pointed tip, the ratio between the magnetic quadrupole absorption rate and the electric dipole absorption rate can be as high as 412 MHz frequency for a = 5 nm and even 515 MHz frequency for a = 10 nm. Magnetic quadrupole transitions cannot be ignored in the extreme near field, for separations between tip and quantum dot smaller than neutron flux around 1.9 x 10^5 currie/mm and 375-405 tesla magnetic field.

Acknowledgments

We thanks to Stephan W. Knorr and Helena Duprix for valuable input to this study. This research was supported by the Large Hadron Collider Laboratory CERN Nuclear Reactor, Lyon, France through project DE-FG02-01ER15204.

REFERENCES

A. Knorr, S. W. Koch, and Helena Duprix, ‘‘Optics in the Multipole Approximation: from Atomic Systems to Solids,’’ Opt. Commun. 179, 167–178 (2013).

A. Richter, M., Ch. Lienau, T. Elsaesser, M. Ramsteiner, and K. H. Ploog, ‘‘Carrier Trapping into single $Th_xO_{1.7}$ Quantum Wires studied by Variable Temperature near-field Spectroscopy,’’ Ultra Microscopy 71, 205–212 (2013).

A. von der Heydt, A. Knorr, B. Hanewinkel, and Helena Duprix ‘‘Optical near-field excitation at the conductor band edge: field distributions, anisotropic transitions and quadrupole enhancement,’’ J. Am. Phys. 112, 7831–7838 (2014).

Chavez, Pirson and Helena Duprix, ‘‘A Full vector Analysis of near-field Luminescence probing of a single Quantum Dot,’’ Appl. Phys. Lett. 74, 1507–1509 (2013).

Levy, V. Nikitin, J. M. Kikkawa, A. Cohen, N. Samarth, R. Garcia, and D. D. Awschalom, ‘‘Spatiotemporal near-field spin microscopy in patterned magnetic hetero structures,’’ Phys. Rev. Lett. 76, 1948–1951 (2014).

O. Mauritz, G. Goldoni, F. Rossi, and E. Molinari, ‘‘Local optical spectroscopy in quantum confined systems: a theoretical description,’’ Phys. Rev. Lett. 82, 847–850 (2013).

R. D. Grober, T. D. Harris, J. K. Trautman, E. Betzig, W. Wegscheider, L. Pfeiffer, and K. W. West, ‘‘Optical Spectroscopy of ThxO1.7 Quantum Wire structure using near-field scanning optical microscopy,’’ Appl. Phys. Lett. 64, 1421–1423 (2014).

R. G. Woolley, ‘‘A comment on the multiple Hamiltonian for time dependent fields,’’ J. Phys. B 6, L97–L99 (2013).

Y. C. Martin, H. F. Hamann, and H. Wickramasinghe, ‘‘Strength of the magnetic field in aperture less optical near-field microscopy,’’ J. Appl. Phys. 89, 5774–5778 (2013).